This is the author's version of an article that has been published in this journal. Changes were made to this version by the publisher prior to publication.
The final version of record is available at http://dx.doi.org/10.1109/TNS.2020.3029730

Electron, neutron and proton irradiation effects on SiC radiation detectors

Joan Marc Rafí, Giulio Pellegrini, Philippe Godignon, Sofía Otero Ugobono, Gemma Rius, Isao Tsunoda, Masashi Yoneoka, Kenichiro Takakura, Gregor Kramberger, and Michael Moll

Abstract—**Owing to their low dark current, high transparency, high thermal conductivity and potential radiation hardness, there is a special interest in silicon carbide devices for radiation monitoring in radiation harsh environments and with elevated temperatures and, especially, for the plasma diagnostic systems in future nuclear fusion reactors. In this work, four-quadrant pn junction diodes produced on epitaxial 4H-SiC substrates are studied. The impact of electron, neutron and proton irradiations (up to fluences of 1x10^{16} e/cm^{2}, 2x10^{15} n/cm^{2} and 2.5x10^{15} p/cm^{2}, respectively) on the electrical characteristics is studied by means of current-voltage (I-V) and capacitance-voltage (C-V) techniques. Relevantly, regardless of particle type and applied fluences, the results show similar low reverse currents for irradiated SiC devices, which are at least about four orders of magnitude lower than comparable Si devices. The effects of irradiation on interquadrant resistance and charge build-up in the interquadrant isolation are assessed. Furthermore, device performance as a radiation detector is investigated upon exposure to a collimated ^{239}Pu-^{241}Am-^{244}Cm tri-alpha source. The performance at room temperature is preserved even for the highest irradiation fluences, and despite the fact that the rectification character in electrical characteristics is lost. From the results, advantages of using SiC devices in alpha particle detection in harsh environments can be envisaged.**

Index Terms—**Semiconductor radiation detectors, Silicon carbide, Radiation effects, Alpha particles, Fusion reactors**

I. Introduction

Semiconductor radiation detectors provide excellent performance in terms of position and energy resolution and they are widely used in high energy physics, space, medical, nuclear, and security applications [1]. Apart from mainstream silicon devices, silicon carbide devices are of special interest for some of these applications because of their wider band gap energy (3.27 eV for 4H-SiC) and higher atomic displacement threshold energy (21 eV for C and 35 eV for Si), providing lower susceptibility to variable temperature and illumination conditions, as well as a potentially higher radiation hardness [2-4]. However, the different SiC polytypes and difficulties in crystal growth had often made it difficult to assess SiC radiation detector properties during the last decades [5,6]. Recently, larger SiC substrates (up to 8-inches diameter wafers) and high quality chemical vapour deposited epitaxial layers have been achieved. SiC is currently considered one of the most attractive semiconductor materials for solid-state detectors in harsh radiation environments and high temperature operation and, in particular, for alpha particle detection in plasma diagnostic systems for future nuclear fusion reactors [7-9].

Segmented silicon photodiodes are very useful devices as X-ray beam monitors in synchrotron radiation beamlines. In order to be used in transmissive mode and given the absorption properties of silicon, the devices must be thinner than 10 μm to achieve X-ray transmission higher than 90% for photon energies above 10 keV [10-12]. Bulk Si segmented devices are also of interest for astronomy and space applications, such as solar tracking systems [13]. Owing to their lower dark current, higher transparency and superior radiation hardness, there is also interest in wider band-gap semiconductors, particularly, diamond and SiC, for these radiation monitoring applications [14-16]. High-quality diamond substrates are, however, costly to obtain and to process. As the X-rays maximum energy transfer to Si or SiC atoms is below the threshold energy for radiation-induced dislocation of the crystalline lattice, no bulk damage is expected for Si or SiC detectors operating in synchrotron beams. However, very high radiation dose rates, in the range of 1 Mrad/s, can be reached and microelectronic devices may still degrade due to generation and trapping of charge in dielectric layers used in their isolation and passivation, as well as surface currents associated with radiation-induced interface traps [17].

Consequently, in recent years, renewed interest in the study of radiation effects on SiC technologies for the envisaged applications has grown. Scattered results from different irradiation sources have been reported in the literature. While most of the published works concentrated on basic Schottky diode structures [8,18-21], others, like the present study, used pn junction diodes [22-24]. As a difference to previous works, here four-quadrant diodes produced on epitaxial SiC are studied, and they are benchmarked to both ultrathin (10 μm-thick) and high resistivity bulk Si devices fabricated with the same design on these different substrates. Radiation hardness of their electrical characteristics is studied by means of electron,

This work has been partially financed by Spanish Ministry of Science, Innovation and Universities through the Nuclear and Particle Physics program project FIS-FPN-RTI2018-094906-B-C22 (MCIU/FEDER UE) and it has received funding from the European Union's Horizon 2020 Research and Innovation programme under Grant Agreement no. 654168 (AIDA-2020). It has been partially performed within a collaborative research project at Nuclear Professional School, School of Engineering, The University of Tokyo (Grant # 20016) and it has made use of the Spanish ICTS Network MICRONANOFABS partially supported by MINECO. G. R. acknowledges RYC-2016-21412.

J.M. Rafí, G. Pellegrini, P. Godignon, S. Otero Ugobono, and G. Rius are with Instituto de Microelectrónica de Barcelona, CNM-CSIC, Campus UAB, 08193 Bellaterra, Barcelona, Spain. (corresponding e-mail: jm.rafi@csic.es).

I. Tsunoda, M. Yoneoka, and K. Takakura are with National Institute of Technology (KOSEN), Kumamoto College, 2659-2 Suya, Kumamoto, Japan.

G. Kramberger is with Jozef Stefan Institute, SI-1000 Ljubljana, Slovenia.

M. Moll is with the European Organization for Nuclear Research (CERN), 1211 Geneva, Switzerland.

Copyright (c) 2020 IEEE. Personal use is permitted. For any other purposes, permission must be obtained from the IEEE by emailing pubs-permissions@ieee.org.

This is the author's version of an article that has been published in this journal. Changes were made to this version by the publisher prior to publication.
The final version of record is available at http://dx.doi.org/10.1109/TNS.2020.3029730

neutron and proton irradiations. Impact of irradiation on interquadrant resistance and charge build-up in the interquadrant isolation is assessed. Finally, device performance as a radiation detector is investigated upon exposure to a collimated ^{239}Pu-^{241}Am-^{244}Cm tri-alpha source.

II. Experimental Details

A. Four-quadrant SiC diodes

Device fabrication was carried out at the IMB-CNM-CSIC cleanroom following well-stablished p-on-n diode processing technologies, and using the same photolithographic mask set, on both high resistivity silicon [25] and silicon carbide substrates [26]. Figure 1 shows the schematic cross section of a four-quadrant diode on the epitaxied SiC substrate, as well as a top view optical microscopy image of a fabricated device. This work mainly concentrates on the results of the Al-implanted pn junction diodes fabricated on a 4H-SiC substrate with a 30 µm-thick n-type epilayer doped at $1.5\text{x}10^{15}$ cm^{-3}. The process included also devices fabricated on high resistivity (2 kΩ·cm) n-type float zone bulk silicon (with 285 µm wafer thickness and 130 V full depletion voltage), as well as on ultrathin (10 µm) silicon films [16], which were obtained by means of direct wafer bonding, wafer thinning, p-on-n device processing and backside deep anisotropic etching [11,12]. The mask layout included single pn junction diodes (i.e., not segmented into four quadrants), with a 3 mm x 3 mm area, and four-quadrant diodes of different space gap between quadrants (defined as “d” in Figure 1(b)), as well as various geometries for the front side metal layer [12,16]. Four-quadrant diodes with interquadrant distance d = 25 µm and metal overlap x = 5 µm (Figure 1(b)) were used for the present work. Furthermore, metal-oxide-semiconductor (MOS) capacitors, using as gate dielectric the interquadrant isolation oxide used for the four-quadrant diode structures, were also included.

B. Irradiations

In order to evaluate the radiation hardness of the devices, some sample sets were subjected to unbiased (the terminals of the devices were left floating) electron, neutron and proton irradiations. Beam direction for all irradiations was perpendicular to the front side of the devices. 2 MeV electron irradiations were carried out at the Takasaki-QST electron accelerator in Takasaki, Japan. Neutron irradiations were performed at the JSI TRIGA research reactor in Ljubljana, Slovenia and 24 GeV/c proton irradiations were carried out at the CERN PS-IRRAD facility in Geneva, Switzerland. The reported hardness factors for nonionizing energy loss (NIEL) in silicon with respect to 1 MeV neutrons are $2.49\text{x}10^{-2}$ for the 2 MeV electrons [27], 0.9 for the JSI neutrons [28] and 0.56 for the 24 GeV/c protons [29,30]. In order to reduce any possible thermal annealing effects of the radiation-induced damage, after irradiation and between measurements, the detectors were stored in a freezer at a temperature of about -25ºC. The shipping of the irradiated samples from the irradiation facility to the measurement laboratory was carried out at below 0ºC temperature in the case of the neutron irradiated devices and at room temperature for 24 hours and two weeks in the case of the proton and electron irradiated samples, respectively.

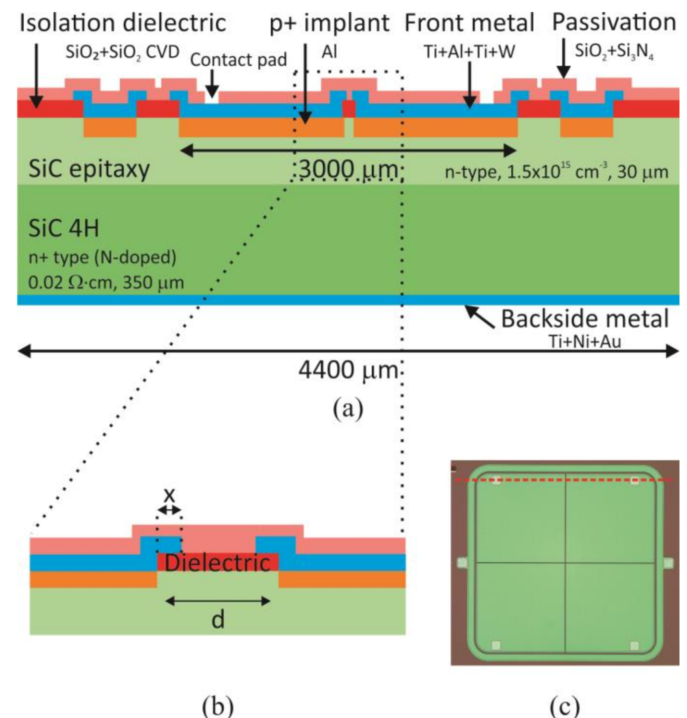

Fig. 1. (a) Schematic cross section (layers and features not drawn to scale) of a four-quadrant diode, including its guard ring, fabricated on epitaxied SiC substrate, (b) detail of a region with the definition of the interquadrant distance “d”, as well as the metal overlapped isolated region “x” and (c) top view optical microscopy image of a fabricated four-quadrant diode. Dashed red line indicates cross section region in (a).

C. Electrical characterization

Current-voltage (I-V) and Capacitance-Voltage (C-V) measurements were carried out at room temperature in a Cascade Summit 11000B-M probe station by using an HP 4155B semiconductor parameter analyser and an Agilent 4284A Precision LCR Meter. C-V measuring frequencies ranged from 0.1 kHz to 1000 kHz. For high voltage I-V measurements a Keithley 2410 SourceMeter was used.

D. Alpha source setup

The set-up for the alpha particle detection included an AmpTek A250 Charge Sensitive Preamplifier, an Ortec 671 Spectroscopy Amplifier and an AmpTek 8000A multichannel analyzer (MCA). The reverse bias was applied with a Keithley 2410.

III. Electrical characterization

A. Current-Voltage characteristics

Figure 2 shows I-V characteristics of epitaxial SiC diodes after different electron, neutron and proton irradiation fluences. As previously observed with electron irradiation results [16], relatively low reverse currents are measured on both neutron and proton irradiated SiC diodes. This is different from the results on bulk silicon and 10 µm-thick Si devices, where about four to six orders of magnitude higher leakage currents are generally observed at room temperature conditions.

Copyright (c) 2020 IEEE. Personal use is permitted. For any other purposes, permission must be obtained from the IEEE by emailing pubs-permissions@ieee.org.

This is the author's version of an article that has been published in this journal. Changes were made to this version by the publisher prior to publication.
The final version of record is available at http://dx.doi.org/10.1109/TNS.2020.3029730

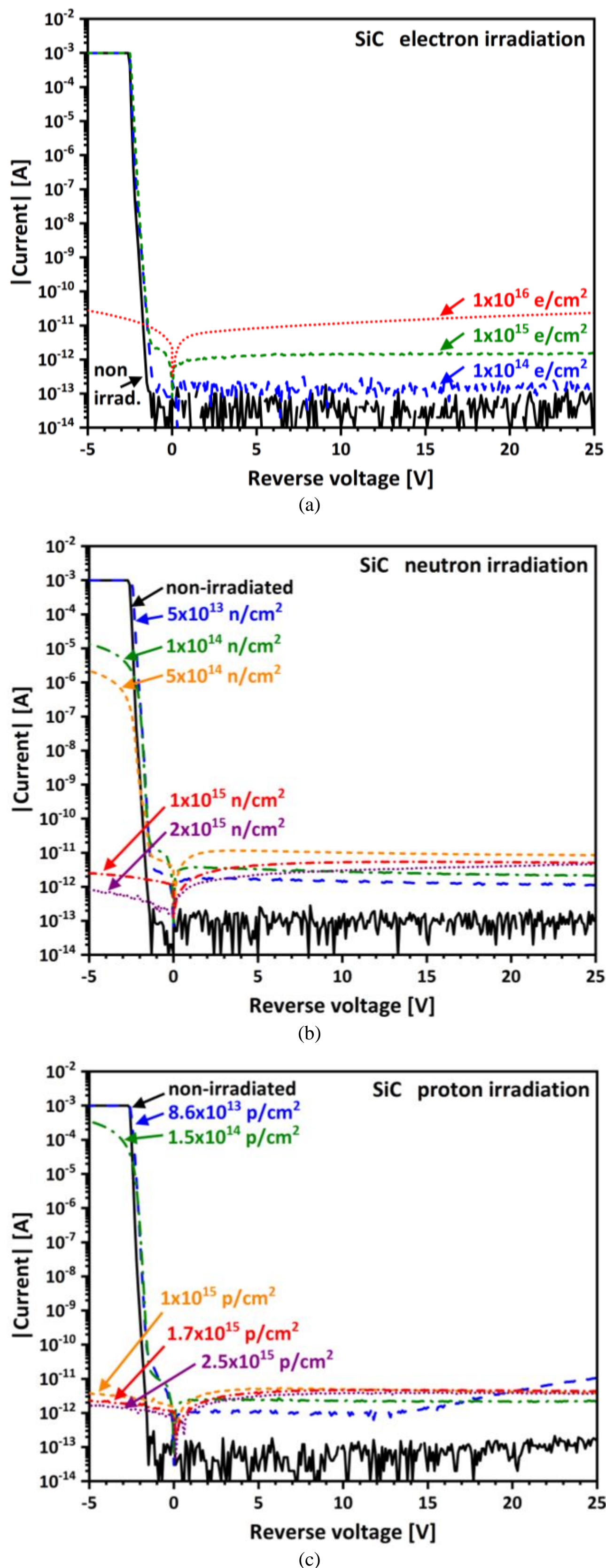

Fig. 2. Diode current-voltage characteristics measured for epitaxial SiC diodes at different (a) electron, (b) neutron and (c) proton irradiation fluences.

Furthermore, as also found on electron-irradiated silicon devices [16], some radiation-induced current decrease in forward operation is observed for SiC devices at intermediate neutron and proton irradiation fluences (between $1x10^{14}$ particles/cm^2 and $1x10^{15}$ particles/cm^2 in figures 2(b) and 2(c)). This behaviour is associated to conduction resistance increase, due to the generation of radiation-induced defects. For the case of Schottky diodes with unipolar conduction, the increase in series resistance has been correlated with a decrease in the effective dopant density, due to carrier removal or doping compensation [31,32]. In the case of pn junction diodes, with bipolar conduction, a similar on-resistance increase after electron irradiation has been recently reported [33]. By means of microwave photoconductivity decay measurements of the epilayers, the degradation has been mainly attributed to carrier recombination lifetime reduction [33], due to the formation of radiation induced deep level defects, such as carbon vacancies (V_C), silicon vacancies (V_{Si}) and V_C+V_{Si} complexes [33,34]. This weakens the conduction modulation in the low doped drift layer, resulting therefore in a remarkable decrease of the forward current [35]. Finally, the rectification character is also lost in the SiC diodes subjected to the highest neutron or proton fluences (above $1x10^{15}$ particles/cm^2) and in the highest electron irradiated SiC devices ($1x10^{16}$ e/cm^2), which is in agreement with previous results on neutron-irradiated pn junction devices at comparable fluences [22-24]. This is indicative of the lightly doped n-type epilayer is also becoming intrinsic after high irradiation fluences [22], similarly to Schottky diodes [34].

The formation of generation-recombination centres is responsible for the increase of the leakage current. Figure 3 shows the reverse current density (I_{vol}) dependence on irradiation fluence at fixed reverse bias conditions (5 V for both, bulk Si and 10 μm-thick Si devices, and 25 V for epitaxial SiC diodes). I_{vol} is defined as the leakage current density of the depleted semiconductor volume: $I_{vol} \equiv I/(\text{area} \times W_{dep})$, where $W_{dep} = (\varepsilon \cdot \text{area})/C$, C is the measured diode capacitance at the fixed reverse bias condition and ε is the semiconductor permittivity [36]. From the Si bulk electron irradiation results, a value of $7.9x10^{-19}$ A/cm is extracted for the leakage current damage rate (α), according to $I_{vol} = \alpha \cdot \phi$, with ϕ being the irradiation fluence. Taking into account the nonionizing energy loss (NIEL) relative hardness factor of the 2 MeV electrons with respect to 1 MeV neutrons, the obtained α value is in the range of reported results for irradiated Si [36]. Importantly, in the case of the electron-irradiated SiC devices, a nearly five orders of magnitude lower value is obtained for the leakage current damage rate $\alpha = 9.2x10^{-24}$ A/cm. The low current levels measured in the irradiated SiC devices may be attributed to a lower creation of damage due to its higher atomic displacement threshold energies [4] and a lower carrier generation in the created defects due to its higher bandgap energy [33].

In the case of bulk Si and 10 μm-thick Si devices subjected to neutron and proton irradiations, an increase of about two orders of magnitude in leakage current is observed for the lowest irradiation fluences ($5x10^{13}$ n/cm^2 and $8.6x10^{13}$ p/cm^2,

Copyright (c) 2020 IEEE. Personal use is permitted. For any other purposes, permission must be obtained from the IEEE by emailing pubs-permissions@ieee.org.

This is the author's version of an article that has been published in this journal. Changes were made to this version by the publisher prior to publication.
The final version of record is available at http://dx.doi.org/10.1109/TNS.2020.3029730

respectively) and some smaller progressive increase is observed for higher neutron and proton irradiation fluences. α values of 3.8×10^{-17} A/cm and 1.6×10^{-17} A/cm have been respectively extracted for the neutron and proton irradiated bulk Si devices, being this also in the range of reported results for irradiated Si [36], when taking into account the corresponding relative hardness factor for the neutrons and protons.

Interestingly, at least about four orders of magnitude lower reverse diode currents are measured in the SiC devices. Some progressive increase of leakage current is observed up to neutron and proton fluences around 1×10^{15} particles/cm^2, where the rectification character in electrical characteristics is lost. Finally, saturation or even a slight dark current decrease can be identified for the highest neutron and proton irradiation fluences, which again is in agreement with previous results on neutron-irradiated pn devices [23,24]. Recently, insignificant changes observed in the reverse leakage current in similar irradiated SiC diodes have been attributed to the 4H-SiC wide bandgap, which supresses the carrier generation from the radiation induced defects [33].

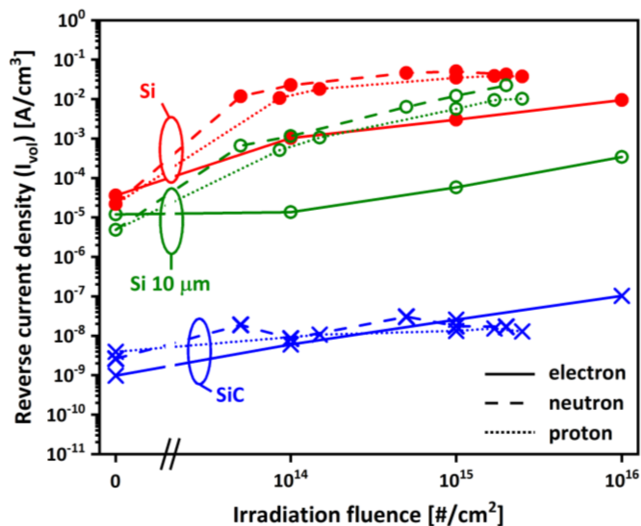

Fig. 3. Reverse current density (I_{vol}) measured for bulk Si, 10 μm-thick Si and for epitaxial SiC diodes at different electron, neutron and proton irradiation fluences (measured at 5 V for both bulk Si and 10 μm-thick Si devices, while at 25 V for epitaxial SiC diodes).

B. Capacitance-Voltage characteristics

Figure 4 shows C-V characteristics measured for epitaxial SiC diodes at different electron irradiation fluences. In agreement with I-V results, diode-like C-V characteristics were only observed in the devices that were irradiated below 1×10^{15} e/cm^2. Similarly, in the cases of the neutron and proton irradiated devices, their characteristics were only preserved for the lowest fluences (up to 5×10^{13} n/cm^2 and 8.6×10^{13} p/cm^2, respectively). Flat C-V curves with fixed capacitance values around 25 pF were obtained for the electron, neutron and proton highest fluences. This common value would be the expected capacitance for a parallel plate capacitor with the diode's area and a distance between the plates of about 30 μm. Similar flat C-V characteristics had already been observed in the case of neutron-irradiated Schottky and pn junction diodes at fluences ranging from 1×10^{14} n/cm^2 to 3×10^{15} n/cm^2. As discussed in the I-V results, this is indicative of the lightly doped n-type epilayer becoming intrinsic after high irradiation fluences, due to compensation by radiation induced acceptor-like defects [22-23].

Figure 5 shows the effective doping concentrations for the epitaxial SiC diodes after the lowest irradiation fluences, where diode-like C-V characteristics allowed the extraction. Extracting a carrier removal rate from the lowest fluence data of the electron, neutron and proton irradiation results in values of 0.72 cm^{-1}, 19.8 cm^{-1} and 9.3 cm^{-1}, respectively. The values dispersion would come into a narrower range when taking into account the radiation hardness factors. However, as pointed in a previous study [32], neutrons seem to be a bit more damaging in SiC than in Si when compared to the high energetic proton damage. The obtained carrier removal rates are in the range of previous estimations for electron and neutron irradiated 4H-SiC Schottky barriers [37,38] (0.35 cm^{-1} and 9.7 cm^{-1}, respectively).

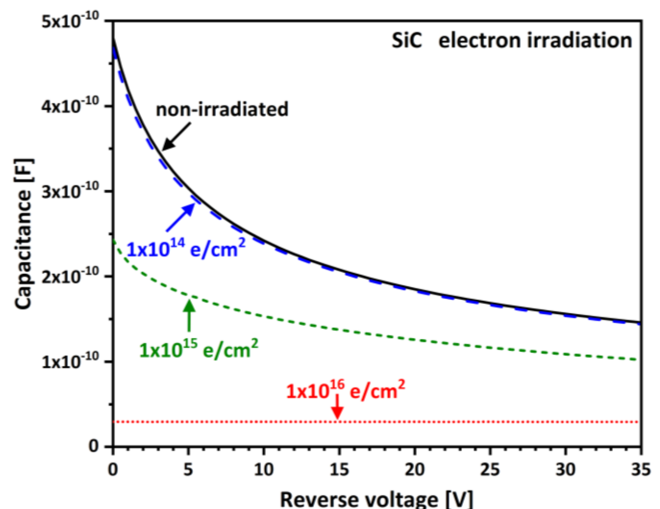

Fig. 4. Capacitance-voltage characteristics measured at 10 kHz for epitaxial SiC diodes at different electron irradiation fluences.

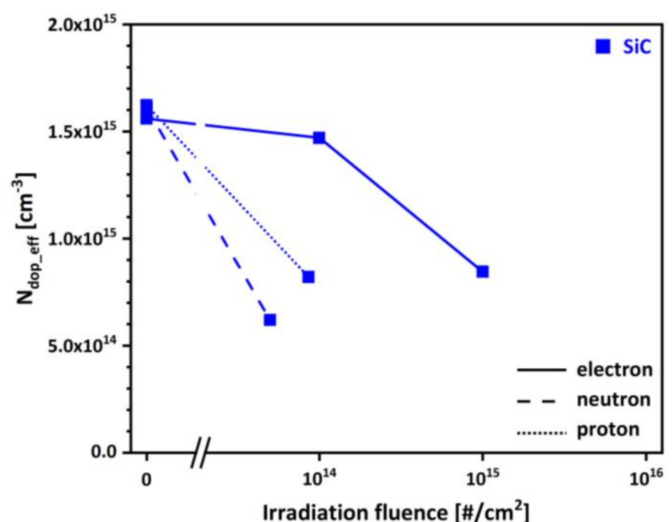

Fig. 5. Extracted effective doping concentration (N_{dop_eff}) (at 5 μm depth) for epitaxial SiC diodes at different (a) electron, (b) neutron and (c) proton irradiation fluences.

Copyright (c) 2020 IEEE. Personal use is permitted. For any other purposes, permission must be obtained from the IEEE by emailing pubs-permissions@ieee.org.

This is the author's version of an article that has been published in this journal. Changes were made to this version by the publisher prior to publication.
The final version of record is available at http://dx.doi.org/10.1109/TNS.2020.3029730

C. Interquadrant resistance

In order to investigate the possible loss of interquadrant isolation upon irradiation, three independent HP 4155B source monitor units (SMUs) were respectively connected to the first quadrant (terminal 1), to the second, third and fourth quadrants shorted together (terminal 2) and to the backside contact (terminal 3). While the first quadrant was kept at zero bias, current versus voltage curves were measured on it (I_1 current measured at terminal 1) when a limited voltage sweep was applied to its three shorted neighbour quadrants (V_2 voltage sweep applied to terminal 2, from -1 V to +1 V and -5 V to +5 V for Si and SiC devices, respectively). These curves were measured for several diode backside reverse voltages (V_3 applied to terminal 3). An estimation of the interquadrant resistance was obtained from the slope of I_1 versus V_2 ($R_{interquadrant}=1/|(dI_1/dV_2)|$). The slopes were obtained by means of linear curve fits of the measured characteristics at the various diode backside reverse biases.

Figure 6 shows the extracted $R_{interquadrant}$ values for bulk Si, 10 μm-thick Si and epitaxial SiC four quadrant diodes at different electron, neutron and proton irradiation fluences. The $R_{interquadrant}$ values correspond to conditions of high reverse bias applied to the substrate (100 V for bulk Si and epitaxial SiC diodes and 10 V for 10 μm-thick Si devices). The highest $R_{interquadrant}$ values are obtained for SiC devices, followed by 10 μm-thick Si and bulk Si devices. A general trend of decreasing $R_{interquadrant}$ values with increasing irradiation was found, with the exception of SiC samples exposed to the highest neutron and proton irradiation fluences, where no rectification characteristics were measured for the devices. Additionally, some saturation in $R_{interquadrant}$ seems to be observed in the Si bulk devices exposed to the highest irradiation fluences.

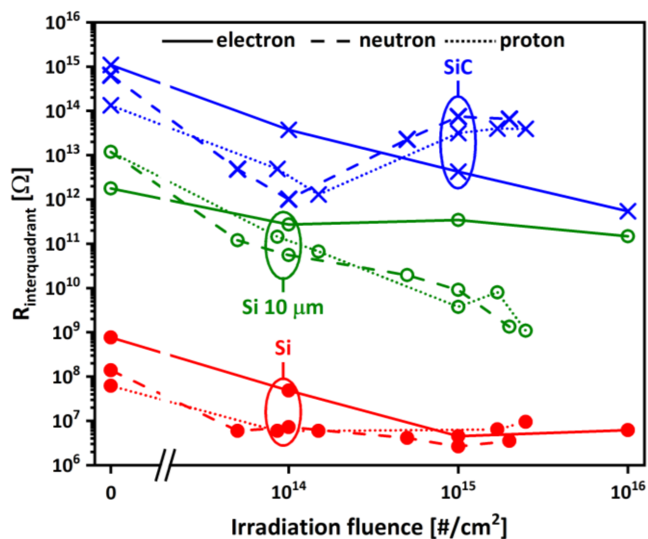

Fig. 6. Extracted $R_{interquadrant}$ for bulk Si, 10 μm-thick Si and epitaxial SiC diodes at different electron, neutron and proton irradiation fluences.

In order to evaluate radiation-induced charge build-up in the diode interquadrant isolation dielectric layer, several MOS capacitors implementing the same oxide as gate dielectric were also irradiated. In the case of both thin film and bulk Si devices, the interquadrant isolation dielectric is composed of a thermally grown SiO_2 layer of 520 nm thickness plus a deposited 180 nm Si_3N_4 layer, which was also used as a mask for the wafer backside thinning process in the case of the 10 μm-thick Si devices. In the case of the SiC devices, the dielectric stack is composed of a 30 nm thermally grown SiO_2 layer plus a 1000 nm thick deposited SiO_2 layer. From the flat band voltage (V_{fb}) shifts of the measured C-V curves, an estimation of the oxide effective trapped charge density (N_{t_eff}), defined as a fixed charge located at the silicon/dielectric interface, has been obtained [39]. It is based on the comparison of the extracted V_{fb} values with the expected figures for an ideal MOS structure. Theoretical V_{fb} values of -0.32 V, -0.16 V and +0.84 V have been used for the non-irradiated MOS capacitors on the bulk Si, 10 μm-thick Si and SiC substrates, respectively. The values are directly derived from the corresponding metal work functions and semiconductor doping concentrations [39].

Figure 7 shows the shift of effective trapped charge densities (ΔN_{t_eff}) corresponding to electron, neutron and proton irradiated MOS capacitors on bulk Si, 10 μm-thick Si and epitaxial SiC substrates. Low N_{t_eff} values, in the range of $+3.5\times10^{10}$ cm^{-2}, -1.4×10^{10} cm^{-2} and -1.9×10^{11} cm^{-2} have been obtained for non-irradiated bulk Si, 10 μm-thick Si and epitaxial SiC MOS devices, respectively. The higher oxide trapped charge densities encountered in SiC/SiO_2 interface, compared to Si/SiO_2, is generally attributed to the larger density of defects associated with the formation of silicon oxycarbide or carbon clusters at or near the interface or intrinsic defects extending from the interface into the oxide layer during the oxidation. This represents a major challenge for the successful fabrication of SiC metal-oxide-semiconductor (MOS) electronic devices [40,41].

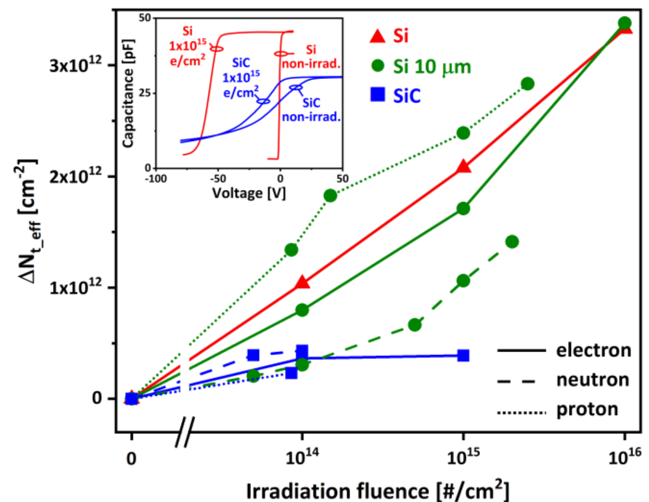

Fig. 7. Shift of effective trapped charge densities in the isolation dielectric (ΔN_{t_eff}), extracted from C-V curves measured at 1 kHz on electron, neutron and proton irradiated MOS capacitors (with area 8.17×10^{-3} cm^2) on bulk Si, 10 μm-thick Si and epitaxial SiC substrates. The inset shows, as an example, C-V curves corresponding to non-irradiated and 1×10^{15} e/cm^2 electron irradiated MOS capacitors on bulk Si and epitaxial SiC substrates.

When subjected to electron irradiation, positive ΔN_{t_eff} values roughly in the range of 1×10^{12} cm^{-2}, 2×10^{12} cm^{-2} and 3.5×10^{12} cm^{-2} are obtained for the silicon devices respectively irradiated to 1×10^{14} e/cm^2, 1×10^{15} e/cm^2 and 1×10^{16} e/cm^2 [16] (with corresponding total ionizing doses of about 2.5 Mrad(Si), 25

Copyright (c) 2020 IEEE. Personal use is permitted. For any other purposes, permission must be obtained from the IEEE by emailing pubs-permissions@ieee.org.

This is the author's version of an article that has been published in this journal. Changes were made to this version by the publisher prior to publication.
The final version of record is available at http://dx.doi.org/10.1109/TNS.2020.3029730

Mrad(Si) and 250 Mrad (Si)). These values are in reasonable agreement with previous results obtained on gamma irradiated 10 µm-thick Si devices [12], when taking into account the equivalent total ionizing dose corresponding to the 2 MeV electron irradiations. For the limited range of results, no saturation in radiation-induced N_{eff} built up has been appreciated for the Si samples. Similar N_{eff} values have been reported for comparable dielectric stacks subjected to high X-ray doses [17], where saturation ΔN_{eff} values in the range of $2x10^{12}$ cm^{-2} to 3.7 $x10^{12}$ cm^{-2} have been finally found at doses in the range of 1 Grad(Si). Interestingly, in the case of the MOS capacitors on the epitaxial SiC substrate, smaller radiation-induced positive charge trapping was observed after $1x10^{14}$ e/cm^2 and $1x10^{15}$ e/cm^2 irradiation. In principle, this could indicate an increased radiation hardness due to their Si_3N_4-free interquadrant isolation stack. Similar to diode I-V and C-V measurements, no functional MOS C-V characteristics could be measured for $1x10^{16}$ e/cm^2 irradiated devices [16]. With regard to neutron and proton irradiation, no N_{t_eff} values could be extracted from the degraded C-V characteristics of irradiated Si bulk and SiC MOS capacitors, obtaining fixed low capacitance flat curves for the highest fluences. Finally, it should be mentioned that similarly to previous gamma [12] and electron irradiation results [16], the observed radiation-induced shifts on 10 µm-Si C-V curves were always higher for lower measurement frequencies, where a larger number of interface and near-interface traps contribute to the measured C-V signal. To conclude, it should be mentioned that the use of device electrical simulation tools could help to clarify the role of the involved geometries, materials and dielectrics, on any possible surface leakage conditions that might determine the observed $R_{interquadrant}$ behaviour.

IV. Alpha Particle Detection

A. Alpha particle spectra

In view of the electrical characterization results obtained on the irradiated SiC diodes, where rectification character was lost for the highest irradiation fluences, device performance as a radiation detector was investigated. When high energy charged particles are delivered to a semiconductor material, collisions and ionization occur, causing the charged particles to lose part of their energy and resulting in the formation of electron and hole pairs. The generated charge carriers drift according to the bias applied to the detector and they can be collected by the electrodes.

Devices were tested in air under the irradiation of a collimated tri-alpha source (^{239}Pu (E_α = 5.245 MeV), ^{241}Am (E_α = 5.486 MeV), ^{244}Cm (E_α = 5.902 MeV), 1.376 kBq). The alpha source and each of the detector devices were enclosed in a metal box, about 8 mm ± 0.5 mm apart from each other. According to SRIM-2013 calculations [42], the experimental dead layer of our measurements (including external air gap, device passivation (50 nm SiO_2 plus 100 nm Si_3N_4) and front metal (a four layer Ti/Al/Ti/W stack with a total thickness of 235 nm)) can absorb about 1.05 MeV ± 0.13 MeV of the incident alpha particles. Thus, their effective kinetic energies to penetrate into the active SiC would be in the range of 4.19 MeV

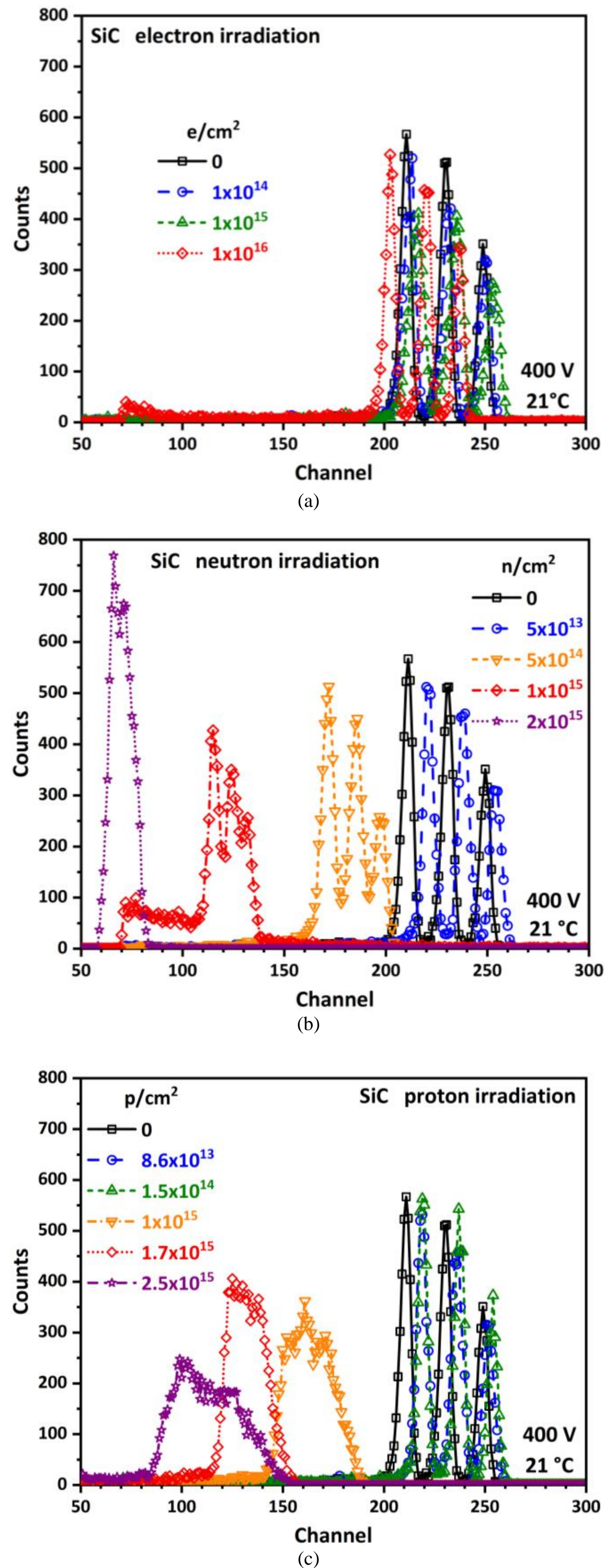

Fig. 8. Response spectra to tri-alpha particles (^{239}Pu, ^{241}Am, ^{244}Cm) for SiC devices at different (a) electron, (b) neutron and (c) proton irradiation fluences. Acquired at a reverse bias voltage of 400 V and room temperature conditions.

Copyright (c) 2020 IEEE. Personal use is permitted. For any other purposes, permission must be obtained from the IEEE by emailing pubs-permissions@ieee.org.

to 4.85 MeV. As the projected range of these alpha particles into the SiC is in the range of 12 µm to 15 µm, which is thinner than the sensitive layer thickness (SiC detector epitaxy), all the remnant energy of the alpha particles is deposited in the active layer.

Figure 8 shows the response spectra of the detectors to the alpha particles emitted by the ^{239}Pu-^{241}Am-^{244}Cm source. The collected counts are plotted as a function of channel number for SiC devices irradiated at different electron, neutron and proton irradiation fluences. The spectra correspond to a fixed reverse bias voltage of 400 V and they were acquired at room temperature conditions (21 ± 1 °C). It is important to highlight that this spectra acquisition at room temperature would not be possible using silicon devices, because of the higher electronic noise originated by the more elevated leakage current levels in irradiated silicon devices. Specifically, for both, non-irradiated and irradiated detectors, the magnitude of the measured leakage current at 400 V reverse bias was in the range of 1 nA, which is within resolution limits of the used high-voltage experimental set-up.

From Figure 8, the three alpha peaks, with centroids around channel numbers 210, 230 and 250, can be clearly resolved in non-irradiated devices. Gaussian functions were used to fit the peaks. Slight spectra shifts are observed for the lowest electron, neutron and proton irradiation fluences (≤ $1x10^{15}$ e/cm^2, ≤ $5x10^{13}$ n/cm^2 and ≤ $1.5x10^{14}$ p/cm^2, respectively). However, they are still in the range of the energy resolution, which can be estimated by the full width at half maximum (FWHM) of the observed peaks.

Interestingly, device capability for alpha particle detection is still observed for the high irradiation fluences where no rectification character is measured on the electrical characteristics. This is the case, for example, of $1x10^{16}$ e/cm^2. However, spectra shift to lower channel numbers is observed after high irradiation fluences. This can already be seen for electron, neutron and proton fluences of $1x10^{16}$ e/cm^2, $5x10^{14}$ n/cm^2 and $1x10^{15}$ p/cm^2, respectively. Furthermore, for the highest neutron and proton irradiation fluences, the peaks broaden and the three alpha peaks cannot be distinguished anymore. Upon irradiation, electrically active defects are formed within the band-gap of the semiconductor and acting as recombination centres or charge traps. Consequently, a reduction in the collected charge is observed as a spectra shift in the channel axis [22,43,44], while a broadening of the alpha peaks due to higher straggling of the incident alpha particles is obtained [23]. Implementing Deep Level Transient Spectroscopy (DLTS) analysis would be of interest to determine the trapping centres which play the main role in the degradation of the different acquired spectra. By means of DLTS, radiation induced point defects, such as carbon vacancy (V_C), silicon vacancy (V_{Si}) and V_C+V_{Si} complexes have been recently identified in similar electron irradiated pn junction diodes [33], together with some other related complexes in neutron irradiated 4H-SiC devices [34].

B. Charge Collection Efficiency

Figure 9 shows the evolution of the peak centroid, also referred as charge collection efficiency (CCE), as a function of

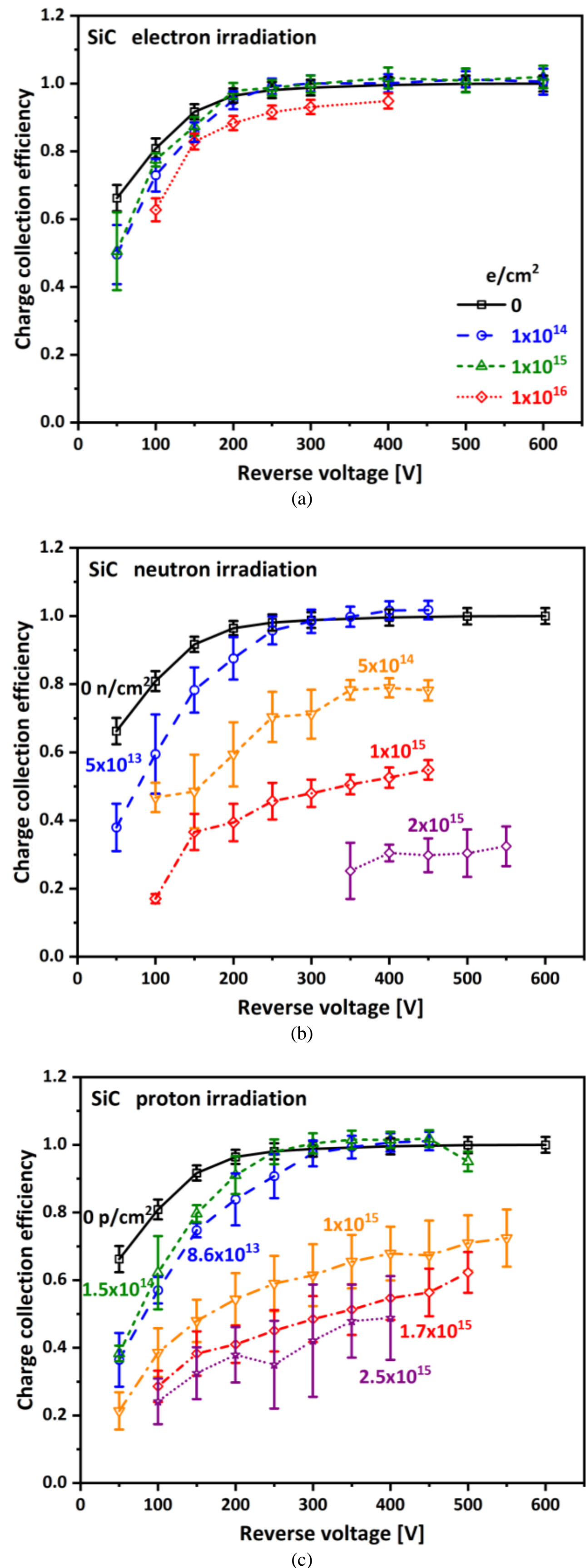

Fig. 9. Charge collection efficiency for SiC devices at different (a) electron, (b) neutron and (c) proton irradiation fluences. Acquired at room temperature conditions.

Copyright (c) 2020 IEEE. Personal use is permitted. For any other purposes, permission must be obtained from the IEEE by emailing pubs-permissions@ieee.org.

This is the author's version of an article that has been published in this journal. Changes were made to this version by the publisher prior to publication.
The final version of record is available at http://dx.doi.org/10.1109/TNS.2020.3029730

reverse bias for the SiC devices at different electron, neutron and proton irradiation fluences. The efficiency curve of non-irradiated detectors reaches saturation at about 250 V, which corresponds to an estimated depletion depth of about 12.5 µm from C-V curves, which is in agreement with the expected active depth for alpha particle detection. With regard to electron irradiation, only small changes can be observed for $1x10^{14}$ e/cm^2 and $1x10^{15}$ e/cm^2, however some significant CCE reduction, in the range of 10%, is found at the highest fluence ($1x10^{16}$ e/cm^2). For the lowest neutron and proton irradiations ($\leq 5x10^{13}$ n/cm^2 and $\leq 1.5x10^{14}$ p/cm^2, respectively), some CCE reduction is observed only at voltages below the plateau, which is observed for these fluences at about 300 V. As the probability of charge trapping is proportional to the drift time of the carriers, the charge collection efficiency can be restored by applying a higher bias voltage, to force shorter drift times.

Finally, the detectors are still operational for the highest irradiation fluences, where no rectification character is observed on the electrical characteristics. However, they need high reverse voltages to avoid the decrease in signal intensity and the CCE does not reach full saturation. For example, the CCE at 400 V decreases in a factor of about 1/2 or 2/3 for fluences of $1x10^{15}$ neutrons/cm^2 or protons/cm^2, respectively. These results are in the range of previous reports observed in the case of neutron-irradiated Schottky and pn junction diodes at similar fluences [20,22].

V. Conclusion

Segmented four-quadrant pn junction diodes have been fabricated on epitaxial SiC, as well as on ultrathin (10 µm) and high resistivity bulk Si substrates. The impact of electron, neutron and proton irradiations on their electrical characteristics has been analysed. The results show low reverse currents for SiC devices subjected to all studied irradiations, with a loss of electrical rectification character for the highest fluences. Impact of irradiation on interquadrant resistance and charge build-up in the interquadrant isolation have been assessed. Interestingly for radiation sensing applications, SiC device performance as a radiation detector is preserved at room temperature for all conditions, as determined by means of irradiation with a tri-alpha source. One interesting aspect for future investigation could be the exploration of thermal annealing treatments of radiation-induced effects in SiC devices.

In summary, the demonstrated superior radiation hardness of silicon carbide devices, as well as their improved performance at elevated temperatures and visible light illumination conditions, may extend their use for some applications beyond the intrinsic limitations of silicon devices. In particular, their advantage for alpha particle detection in plasma diagnostic systems for future nuclear fusion reactors is envisioned.

References

[1] G. Lutz, *Semiconductor radiation detectors*, 2nd ed. Berlin Heidelberg, Germany: Springer-Verlag, 2007.

[2] M. R. Werner, and W. R. Fahrner, "Review on materials, microsensors, systems, and devices for high-temperature and harsh-environment applications," *IEEE Trans. Ind. Electron.*, vol. 48, no. 2, pp. 249-257, 2001, doi: 10.1109/41.915402.

[3] J. B. Casady, and R. W. Johnson, "Status of silicon carbide (SiC) as a wide-bandgap semiconductor for high-temperature applications: a review," *Solid-State Electron.*, vol. 39, no. 10, pp. 1409-1422, 1996, doi: 10.1016/0038-1101(96)00045-7.

[4] F. Nava, G. Bertuccio, A. Cavallini, and E. Vittone, "Silicon carbide and its use as a radiation detector material," *Meas. Sci. Technol.*, vol. 19, 102001, 2008, doi: 10.1088/0957-0233/19/10/102001.

[5] P. J. Sellin, and J. Vaitkus, "New materials for radiation hard semiconductor detectors," *Nucl. Instrum. Methods Phys. Res., Sect. A*, vol. 557, pp. 479-489, 2006, doi: 10.1016/j.nima.2005.10.128.

[6] A. A. Lebedev, A. M. Ivanov, and N. B. Strokan, "Radiation resistance of SiC and nuclear-radiation detectors based on SiC films," *Semiconductors*, vol. 38, no. 2, pp. 125-147, 2004, doi: 10.1134/1.1648363.

[7] S. J. Zweben, R. V. Budny, D. S. Darrow, S. S. Medley, R. Nazikian, B. C. Stratton, E. J. Sydnakowski, and G. Taylor, "Alpha particle physics experiments in the Tokamak fusion test reactor," *Nucl. Fusion*, vol. 40, no. 1, pp. 91-149, doi: 10.1088/0029-5515/40/1/307.

[8] L. Liu, A. Liu, S. Bai, L. Lv, P. Jin, and X. Ouyang, "Radiation resistance of silicon carbide schottky diode detectors in D-T fusion neutron detection," *Sci. Rep.*, vol. 7, 13376, 2017, doi: 10.1038/s41598-017-13715-3.

[9] S. Tudisco, F. La Via, C. Agodi, et al., "SiCILIA-Silicon carbide detectors for intense luminosity investigations and applications," *Sensors*, vol. 18, pp. 2289, 2018, doi: 10.3390/s18072289.

[10] M. R. Fuchs, K. Holldack, M. Bullough, S. E. Walsh, C. Wilburn, A. Erko, F. Schaefers, U. R. Müller, "Transmissive x-ray beam position monitors with submicron position- and submillisecond time resolution," *Rev. Sci. Instrum.*, vol. 79, 063103, 2008, doi: 10.1063/1.2938400.

[11] C. Cruz, G. Jover-Manas, O. Matilla, et al., "10 µm thin transmissive photodiode produced by ALBA Synchrotron and IMB-CNM-CSIC," *J. Instrum.*, vol. 10, C03005, 2015, doi: 10.1088/1748-0221/10/03/C03005.

[12] J. M. Rafí, G. Pellegrini, D. Quirion, S. Hidalgo, P. Godignon, O. Matilla, J. Juanhuix, A. Fontserè, B. Molas, D. Pothin, and P. Fajardo, "10 µm-thick four-quadrant transmissive silicon photodiodes for beam position monitor application: electrical characterization and gamma irradiation effects," *J. Instrum.*, vol. 12, C01004, Jan. 2017, doi: 10.1088/1748-0221/12/01/C01004.

[13] P. Roth, A. Georgiev, and H. Boudinov, Design and construction of a system for sun-tracking, *Renewable Energy*, vol. 29, pp. 393-402, 2004, doi: 10.1016/S0960-1481(03)00196-4.

[14] J. Morse, B. Solar, and H. Graafsma, "Diamond X-ray beam-position monitoring using signal readout at the synchrotron radiofrequency," *J. Synchrotron Radiat.*, vol. 17, pp. 456-464, 2010, doi: 10.1107/S0909049510016547.

[15] S. Nida, A. Tsibizov, T. Ziemann, J. Woerle, A. Moesch, C. Schulze-Briese, C. Pradervand, S. Tudisco, H. Sigg, O. Bunk, U. Grossner, and M. Camarda, "Silicon carbide X-ray beam position monitors for synchrotron applications," *J. Synchrotron Radiat.*, vol. 26, pp. 28-35, 2019, doi: 10.1107/S1600577518014248.

[16] J. M. Rafí, G. Pellegrini, P. Godignon, D. Quirion, S. Hidalgo, O. Matilla, A. Fontserè, B. Molas, K. Takakura, I. Tsunoda, M. Yoneoka, D. Pothin, and P. Fajardo, "Four-quadrant silicon and silicon carbide photodiodes for beam position monitor applications: electrical characterization and electron irradiation effects," *J. Instrum.*, vol. 13, C01045, Jan. 2018, doi: 10.1088/1748-0221/13/01/C01045.

[17] R. Klanner, E. Fretwurst, I. Pintilie, J. Schwandt, J. Zhang, "Study of high-dose X-ray radiation damage of silicon sensors," *Nucl. Instrum. Methods Phys. Res., Sect. A*, vol. 732, pp. 117-121, 2013, doi: 10.1016/j.nima.2013.05.131.

[18] S. Sciortino, F. Hartjes, S. Lagomarsino, F. Nava, M. Brianzi, V. Cindro, C. Lanzieri, M. Moll, and P. Vanni, "Effect of heavy proton and neutron irradiations on epitaxial 4H-SiC Schottky diodes," *Nucl. Instrum. Methods Phys. Res., Sect. A*, vol. 552, pp. 138-145, 2005, doi: 10.1016/j.nima.2005.06.017.

[19] J. Wu, Y. Jiang, J. Lei, X. Fan, Y. Chen, M. Li, D. Zou, and B. Liu, "Effect of neutron irradiation on charge collection efficiency in 4H-SiC Schottky diode," *Nucl. Instrum. Methods Phys. Res., Sect. A*, vol. 735, pp. 218-222, 2014, doi: 10.1016/j.nima.2013.09.041.

[20] F. Nava, P. Vanni, M. Bruzzi, S. Lagomarsino, S. Sciortino, G. Wagner, and C. Lanzieri, "Minimum ionizing and alpha particles

Copyright (c) 2020 IEEE. Personal use is permitted. For any other purposes, permission must be obtained from the IEEE by emailing pubs-permissions@ieee.org.

This is the author's version of an article that has been published in this journal. Changes were made to this version by the publisher prior to publication.
The final version of record is available at http://dx.doi.org/10.1109/TNS.2020.3029730

detectors based on epitaxial semiconductor silicon carbide," *IEEE Trans. Nucl. Sci.*, vol. 51, no. 1, pp. 238-243, 2004, doi: 10.1109/TNS.2004.825095.

[21] F.H. Ruddy, A.R. Dulloo, J.G. Seidel, S. Seshadri, and L.B. Rowland, "Development of a Silicon Carbide Radiation Detector," *IEEE Trans. Nucl. Sci.*, vol. 45, no. 3, pp. 536-541, 1998, doi: 10.1109/23.682444.

[22] F. Moscatelli, A. Scorzoni, A. Poggi, M. Bruzzi, S. Sciortino, S. Lagomarsino, G. Wagner, I. Mandic, and R. Nipoti, "Radiation hardness after very high neutron irradiation of minimum ionizing particle detectors based on 4H-SiC p+n junctions," *IEEE Trans. Nucl. Sci.*, vol. 53, no. 3, pp. 1557-1563, Jun. 2006, doi: 10.1109/TNS.2006.872202.

[23] L. Liu, F. Li, S. Bai, P. Jin, X. Cao and X. Ouyang, "Silicon carbide PIN diode detectors used in harsh neutron irradiation," *Sens. Actuators, A*, vol. 280, pp. 245-251, 2018, doi: 10.1016/j.sna.2018.07.053.

[24] L. Liu, X. Ouyang, J.-L. Ruan, S. Bai, and X.-P. Ouyang, "Performance comparison between SiC and Si neutron detectors in deuterium-tritium fusion neutron irradiation," *IEEE Trans. Nucl. Sci.*, vol. 66, no. 4, pp. 737-741, 2019, doi: 10.1109/TNS.2019.2901797.

[25] M. Lozano, G. Pellegrini, C. Fleta, et al., "Comparison of Radiation Hardness of P-in-N, N-in-N, and N-in-P Silicon Pad Detectors," *IEEE Trans. Nucl. Sci.*, vol. 52, no. 5, pp. 1468-1473, Oct. 2005, doi: 10.1109/TNS.2005.855809.

[26] P. Godignon, X. Jordà, M. Vellvehi, X. Perpiñà, V. Banu, D. López, J. Barbero, P. Brosselard, and S. Masseti, "SiC Schottky Diodes for Harsh Environment Space Applications," *IEEE Trans. Ind. Electron.,* vol. 58, no. 7, pp. 2582-2590, Jul. 2011, doi: 10.1109/TIE.2010.2080252.

[27] G. P. Summers, E. A. Burke, P. Shapiro, S. R. Messenger, and R. J. Walters, "Damage correlations in semiconductors exposed to gamma, electron and proton radiations," *IEEE Trans. Nucl. Sci.*, vol. 40, no. 6, pp. 1372-1379, 1993, doi: 10.1109/23.273529.

[28] Advanced European Infrastructures for Detectors at Accelerators (AIDA2020). *JSI TRIGA reactor Facility*. Accessed: Oct. 22, 2019. [Online]. Available: http://aida2020.web.cern.ch/content/jsi.

[29] CERN. *PS IRRAD Proton Facility*. Accessed: Oct. 22, 2019. [Online]. Available: https://ps-irrad.web.cern.ch/.

[30] I. Mateu, et al. (Jun. 2016). *NIEL Hardness Factor Determination for the New Proton Irradiation Facility at CERN*. [Online]. Available: https://cds.cern.ch/record/2162852.

[31] R. D. Harris, A. J. Frasca, and M. O. Patton, "Displacement damage effects on the forward bias characteristics of SiC Schottky barrier power diodes," *IEEE Trans. Nucl. Sci.*, vol. 52, no. 6, pp. 2408-2412, 2005, doi: 10.1109/TNS.2005.860730.

[32] J. A. Kulisek, and T. E. Blue, "Carrier-removal comparison (n/p) and functional testing of Si and SiC power diodes," *IEEE Trans. Nucl. Sci.*, vol. 57, no. 5, pp. 2906-2914, 2010, doi: 10.1109/TNS.2010.2056931.

[33] P. Dong, Y. Qin, X. Yu, X. Xu, Z. Chen, L. Li, and Y. Cui, "Electron radiation effects on the 4H-SiC PiN diodes characteristics: an insight from point defects to electrical degradation," *IEEE Access*, vol. 7, pp. 170385-170391, 2019, doi: 10.1109/ACCESS.2019.2955385.

[34] F. Nava, A. Castaldini, A. Cavallini, P. Errani, and V. Cindro, "Radiation detection properties of 4H-SiC Schottky diodes irradiated up to 1016 n/cm^2 by 1 MeV Neutrons," *IEEE Trans. Nucl. Sci.*, vol. 53, no. 5, pp. 2977-2982, 2006, doi: 10.1109/TNS.2006.882777.

[35] K. Kaji, H. Niwa, J. Suda, T. Kimoto, "Ultrahigh-voltage SiC p-i-n diodes with improved forward characteristics," *IEEE Trans. Electron Devices*, vol. 62, pp. 374-381, 2015, doi: 10.1109/TED.2014.2352279.

[36] G. Lindström, et al., "Radiation hard silicon detectors - Developments by the RD48 (ROSE) collaboration," *Nucl. Instrum. Methods Phys. Res., Sect. A*, vol. 466, no. 2, pp. 308-326, 2001, doi: 10.1016/S0168-9002(01)00560-5.

[37] P. Hazdra, and J. Bovecký, "Radiation Defects Created in n-Type 4H-SiC by Electron Irradiation in the Energy Range of 1–10 MeV," *Phys. Status Solidi A*, vol. 216, pp. 1900312, 2019, doi: 10.1002/pssa.201900312.

[38] S. Seshadri, A. R. Dulloo, F. H. Ruddy, J. G. Seidel, and L. B. Rowland, "Demonstration of an SiC neutron detector for high-radiation environments," *IEEE Trans. Electron Devices*, vol. 46, no. 3, pp. 567-571, 1999, doi: 10.1109/16.748878.

[39] D. K. Schroder, *Semiconductor material and device characterization*, 3rd ed. Hoboken, NJ, USA: John Wiley & Sons, 2006, pp. 334-335.

[40] A. Pérez-Tomás, P. Godignon, N. Mestres, R. Pérez, J. Millán, "A study of the influence of the annealing processes and interfaces with deposited SiO2 from tetra-ethoxy-silane for reducing the thermal budget in the gate definition of 4H–SiC devices," *Thin Solid Films*, vol. 513, pp. 248-252, 2020, doi: 10.1016/j.tsf.2005.12.308.

[41] M. Cabello, V. Soler, G. Rius, J. Montserrat, J. Rebollo, P. Godignon, "Advanced processing for mobility improvement in 4H-SiC MOSFETs: A review," *Mater. Sci. Semicond. Process.*, vol. 78, pp. 22-31, 2018, doi: 10.1016/j.mssp.2017.10.030.

[42] J. F. Ziegler, M. D. Ziegler, and J. P. Biersack, "SRIM – The stopping and range of ions in matter (2010)," *Nucl. Instrum. Methods Phys. Res., Sect. B*, vol. 268, pp. 1818-1823, 2010, doi: 10.1016/j.nimb.2010.02.091.

[43] F. Nava, E. Vittone, P. Vanni, P.G. Fuochi, and C. Lanzieri, "Radiation tolerance of epitaxial silicon carbide detectors for electrons and γ-rays," *Nucl. Instrum. Methods Phys. Res., Sect. A*, vol. 514, pp. 126-134, 2003, doi: 10.1016/j.nima.2003.08.094.

[44] F. Nava, E. Vittone, P. Vanni, G. Verzellesi, P. G. Fuochi, C. Lanzieri, and M. Glaser, "Radiation tolerance of epitaxial silicon carbide detectors for electrons, protons and gamma-rays," *Nucl. Instrum. Methods Phys. Res., Sect. A*, vol. 505, pp. 645-655, 2003, doi: 10.1016/S0168-9002(02)01558-9.

Copyright (c) 2020 IEEE. Personal use is permitted. For any other purposes, permission must be obtained from the IEEE by emailing pubs-permissions@ieee.org.